JPE 15-5-21

http://dx.doi.org/10.6113/JPE.2015.15.5.1348
ISSN(Print): 1598-2092 / ISSN(Online): 2093-4718

Coordinated Control Strategies with and without Circulating Current in Unified Power Quality Conditioners

Xing-tian Feng† and Zhi-hua Zhang*

†,*College of Information and Control Engineering, China University of Petroleum, Qingdao, China

Abstract

Under traditional unified power quality conditioner (UPQC) control, a UPQC series converter (SC) is mainly used to handle grid-side power quality problems while its parallel converter (PC) is mainly used to handle load-side power quality problems. The SC and PC are relatively independent. The SC is usually in standby mode and it only runs when the grid voltage abruptly changes. In this paper, novel UPQC coordinated control strategies are proposed which use the SC to share the reactive power compensation function of the PC especially without grid-side power quality problems. However, in some cases, there will be a circulating current between the SC and the PC, which will probably influence the compensation fashion, the compensation capacity, or the normal work of the UPQC. Through an active power circulation analysis, strategies with and without a circulating current are presented which fuses the reactive power allocation strategy of the SC and the PC, the composite control strategy of the SC and the compensation strategy of the DC storage unit. Both of the strategies effectively solve the SC long term idle problem, limit the influence of the circulating current, optimize all of the UPQC units and reduce the production cost. An analysis, along with simulation and experimental results, is presented to verify the feasibility and effectiveness of the proposed control strategies.

Key words: Circulating current, Coordination control, Optimization condition, Power allocation, Reactive power compensation, Super-capacitor energy storage, Unified power quality conditioner

I. INTRODUCTION

The integration of distribution generation (DG) sources and the grid is considered as the main method to save investment, reduce energy consumption, and improve both the reliability and flexibility of power systems. The power flows of distribution networks are from one direction to multi-directions due to the joining of lots of DGs. When the power of DGs fluctuates, it leads to some kinds of power quality problems. The development of custom power technology (CPT) provides methods to effectively solve power quality problems. As one type of CPT equipment, the UPQC combines series voltage compensation theory with parallel current compensation theory, which can deal with the asymmetry and harmony of the grid-side voltage and the asymmetry and harmony of the load-side current [1]-[7].

Manuscript received Aug. 2, 2014; accepted Apr. 24, 2015
Recommended for publication by Associate Editor Hao Ma.
†Corresponding Author: topfxt@163.com
Tel: +86-0532-86983023, Fax: +86-0532-86981335, UPC
*Coll. of Information & Control Eng., China Univ. of Petroleum, China

Under the traditional UPQC control, the SC solves grid-side power quality problems, while the PC solves load-side power quality problems. The SC and PC exchange power with the common DC unit, but their functions are relatively independent [8]-[15]. In fact, the SC is mainly in standby mode, and it runs only when there are sudden grid-side power quality problems like voltage sags or swells. Meanwhile, the PC simultaneously fulfills reactive power compensation and harmonic elimination and is usually in heavy-load status. Nowadays, control strategy research on UPQC capacity allocation is usually limited to the case of voltage sags [16]-[19]. There are few references on the capacity allocation between the SC and the PC when the grid voltage is normal. The minimum energy compensation method and the complete compensation method can realize active and reactive power output in series power quality compensation equipment [20]-[22]. In UPQC systems, the SC and PC can coordinate each other. The SC outputs reactive power to share the reactive power compensation function of the PC, which can realize the UPQC coordination control [23]-[25]. [23] and [24] introduce the same strategy which uses a series inverter to

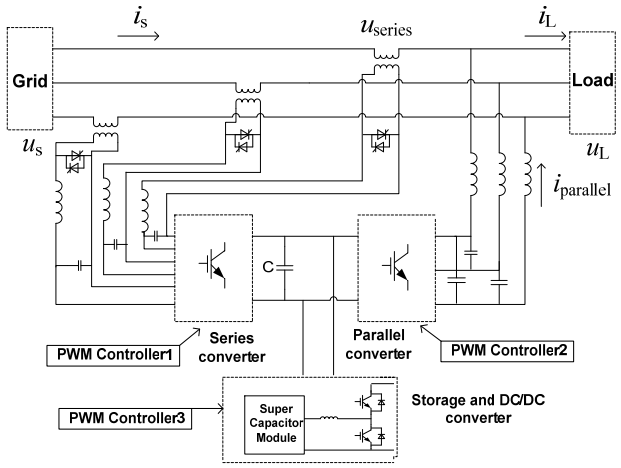

Fig. 1. System structure diagram of UPQC.

realize reactive power compensation. [25] presents a combinatory UPQC and SFCLs (superconducting fault current limiters) to reduce the UPQC cost, and it does not use the UPQC itself to solve the cost problem. None of them consider the circulating power problem. However, the reactive power output of the SC is accompanied by the active power output, which leads to an active power circulating current. The circulating current will unavoidably influence the UPQC capacity. It can also harm the UPQC series converter and parallel converter.

This paper analyzes the active circulating power and proposes a UPQC power flow coordinated control strategy based on the circulating current. This strategy changes the working condition of the SC and PC, reasonably allocates the power output of the SC and PC, utilizes the SC to alleviate the reactive power compensation burden of the PC especially in the case of normal grid voltage, realizes coordinated control of the SC and PC, and improves the power quality problems in distribution networks. The simulation and experimental results testify that the strategy is accurate, reliable, reasonable and adaptable.

II. PROPOSED UPQC STRUCTURE

The UPQC main circuit structure is mainly composed of the SC, the PC, and the common DC unit in Fig. 1. The SC and PC are common 3-phase inverters. The SC connects the grid-side with the series transformer and the thyristor module. The PC connects the load-side with the inductance. The common DC unit includes the storage and the DC/DC converter and the SCM (Super Capacitor Module) constitutes the storage unit.

The SC mainly solves the grid-side voltage quality problems including voltage sags, swells, interruptions, imbalances and so on. The PC mainly solves the load-side current quality problems including reactive power compensation, current harmonics, imbalances, and so on. Finally, the UPQC realizes the load-side voltage u_L sine characteristic, the grid-side current is sine characteristic and the high power factor characteristic (The angle between u_s and i_s is small enough). The series transformer isolates the SC and the grid. The thyristor module provides a by-pass circuit. The storage and DC/DC converter fulfill the reactive power buffer, the energy transfer, the compensation energy provision; and make the SC and PC decouple and solve the voltage interruption problem which the traditional UPQC cannot fully handle. PWM Controller1, PWM Controller2 and PWM Controller3 are used to control the output of the three converters, which will be shown in detail in Fig. 5(b).

III. UPQC COORDINATED CONTROL STRATEGY WITH A CIRCULATING CURRENT

The UPQC coordinated control strategy explores the power output relationship between the SC and PC to alleviate the reactive power compensation burden of the PC. It solves many power quality problems and realizes the coordinated control of the SC and PC. The following analyzes the UPQC coordinated control strategy based on the circulating current theory and takes a single phase as an example.

A. Normal Grid Voltage Analysis

When the grid voltage is normal, the SC outputs reactive power. However, the SC outputs active power at the same time. Fig. 2(a) shows a working vectogram of the UPQC at present. φ is the power factor angle of the resistive and inductive load; $\dot{U}_s$, $\dot{U}_L$ and $\dot{U}_{series}$ are the grid voltage vector, the load voltage vector and the SC output voltage vector respectively; $\dot{I}_L$ and $\dot{I}_L'$ are the load current vector before and after compensation, and they can be decomposed to $\dot{I}_c$ and $\dot{I}_s$, $\dot{I}_c'$ and $\dot{I}_s'$ respectively; the vector direction of $\dot{I}_L'$ can adjust between $\dot{I}_L$ and $\dot{I}_s$, and the vector direction of $\dot{U}_L$ follows; and $\dot{I}_{parallel}$ is the compensation current vector of the PC output.

In Fig. 2(a),

$$\varphi = \gamma + \delta \tag{1}$$

Define the following:

$$\left|\dot{U}_s\right| = \left|\dot{U}_L\right| = U \tag{2}$$

$$\left|\dot{I}_L'\right| = \left|\dot{I}_L\right| = I \tag{3}$$

The SC output voltage vector $\dot{U}_{series}$ is obtained as:

$$\begin{aligned} \dot{U}_{series} &= \left|\dot{U}_{series}\right| \angle \beta \\ &= 2\left|\dot{U}_s\right| \sin\frac{\gamma}{2} \angle (90^0 + \frac{\gamma}{2}) \\ &= 2U \sin\frac{\gamma}{2} \angle (90^0 + \frac{\gamma}{2}) \end{aligned} \tag{4}$$

The active power P_{series} is derived as:

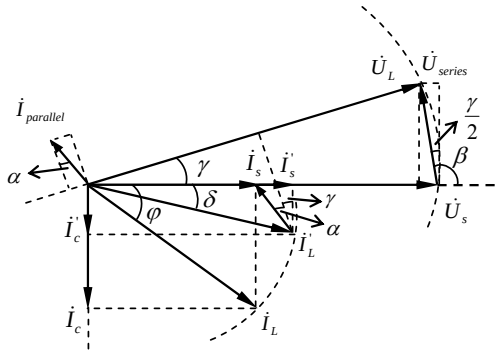

(a) Without voltage sags.

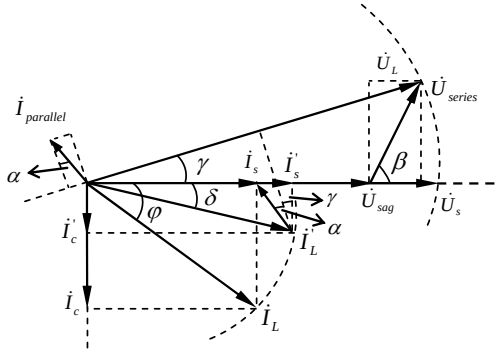

(b) With voltage sags.

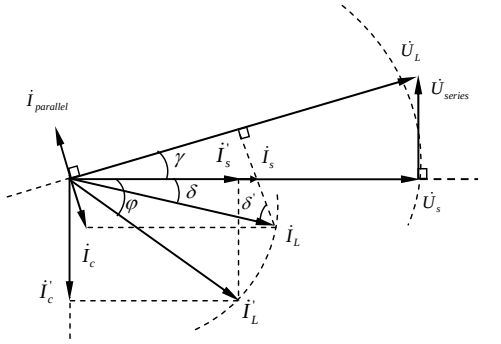

(c) Without circulating current.

Fig. 2. Working vectogram of UPQC.

$$\begin{aligned} P_{series} &= 2U \sin\frac{\gamma}{2}\sin\frac{\gamma}{2}\cdot\left|\dot{I}_L\right|\cos\varphi \\ &= UI(1-\cos\gamma)\cos\varphi \end{aligned} \tag{5}$$

The reactive power Q_{series} is derived as:

$$\begin{aligned} Q_{series} &= 2U \sin\frac{\gamma}{2}\cos\frac{\gamma}{2}\cdot\left|\dot{I}_L\right|\cos\varphi \\ &= UI\sin\gamma\cos\varphi \end{aligned} \tag{6}$$

The PC output current vector $\dot{I}_{parallel}$ is obtained as:

$$\begin{aligned} \dot{I}_{parallel} &= \sqrt{I^2(\cos\delta-\cos\varphi)^2+(I\sin\delta)^2}\angle(90^0+\alpha') \\ &= mI\angle(90^0+\alpha') \end{aligned} \tag{7}$$

Where:

$$\alpha' = \alpha+\gamma = \arctan\frac{I(\cos\delta-\cos\varphi)}{I\sin\delta} = \arctan\frac{\cos\delta-\cos\varphi}{\sin\delta}$$

$$m = \sqrt{(\cos\delta-\cos\varphi)^2+\sin^2\delta}$$

The active power $P_{parallel}$ is derived as:

$$\begin{aligned} P_{parallel} &= U\cdot mI\sin\alpha \\ &= mUI\sin(\alpha'-\gamma) \\ &= mUI(\sin\alpha'\cos\gamma-\cos\alpha'\sin\gamma) \\ &= UI(m\sin\alpha'\cos\gamma-m\cos\alpha'\sin\gamma) \\ &= UI[(\cos\delta-\cos\varphi)\cos\gamma-\sin\delta\sin\gamma] \\ &= UI(\cos\varphi-\cos\gamma\cos\varphi) \\ &= UI(1-\cos\gamma)\cos\varphi \end{aligned} \tag{8}$$

The reactive power $Q_{parallel}$ is derived as:

$$\begin{aligned} Q_{parallel} &= U\cdot mI\cos\alpha \\ &= mUI\cos(\alpha'-\gamma) \\ &= UI(m\cos\alpha'\cos\gamma+m\sin\alpha'\sin\gamma) \\ &= UI[\sin\delta\cos\gamma+(\cos\delta-\cos\varphi)\sin\gamma] \\ &= UI(\sin\varphi-\sin\gamma\cos\varphi) \end{aligned} \tag{9}$$

From Fig. 2(a) and eq. (5), (6), (8), (9), it can be deduced that the SC and PC provide reactive power simultaneously, the SC consumes active power P_{series} from the grid, and the PC generates active power $P_{parallel}$ and P_{series}=$P_{parallel}$. In this way, there is a circulating current between the SC and PC which is up to P_{series} or $P_{parallel}$. The circulating current does not influence the UPQC when it is relatively small (usually less than 10% of the system rated current). In real working processes, the SC and PC capacity can be properly adjusted according to the spot requirements. If the distribution relationship is not suitable, the circulating current is large enough to injure the series and parallel converters. In order to balance the SC and PC capacity, assume that Q_{series}=$Q_{parallel}$, and that the basic condition of the UPQC coordinated control can be derived by:

$$UI\sin\gamma\cos\varphi = UI(\sin\varphi-\sin\gamma\cos\varphi) \tag{10}$$

Usually, $\varphi\in(0,\frac{\pi}{4})$, and the present condition is given as:

$$\gamma_{ref} = \arcsin(\frac{1}{2}\tan\varphi) \tag{11}$$

The circulation ratio is defined as P_{series}/UI or $P_{parallel}$/UI. It can be concluded that the ratio decreases with a decrease of the angle φ from (5) and (11) and that the circulation current is allowed to exist under effective control.

The sum of Q_{series} and $Q_{parallel}$ can be obtained by (12) which is just about the reactive power requirement of the loads.

$$\begin{aligned} Q &= Q_{series}+Q_{parallel} \\ &= UI\sin\gamma\cos\varphi+UI(\sin\varphi-\sin\gamma\cos\varphi) \\ &= UI\sin\varphi \end{aligned} \tag{12}$$

The active power output of the grid can be obtained by (13) which is just about the active power requirement of the loads.

$$P = UI\cos\varphi \tag{13}$$

Under the UPQC coordinated control, when $\varphi=\pi/4$, $\gamma=\pi/6$. In addition, the SC output reactive power is 0.354UI, as does the PC; the circulation active power is 0.095UI; the capacity of the SC or the PC is 0.366UI which shows that the

circulation power is relatively low. When the PC compensates the reactive power alone, the required capacity is 0.707*UI*. Therefore, the strategy decreases the PC capacity and reduces the equipment cost. In addition, the SC is always in the working status which is propitious to timely compensation when voltage quality problems occur.

B. Grid Voltage Sag Analysis

The storage and DC/DC converter provides active power when the voltage sags, and the active current $\dot{I}_s$ can be invariant. In order to transit freely and avoid current impulses, the angle γ_{ref} should keep invariant, which is realized by changing the output voltage vector of the SC. The vectogram is shown as Fig. 2(b). $\dot{U}_{sag}$ is the voltage after sags. Fig. 2(b) shows that the reactive power of both the SC and the PC is invariant; the reactive power distribution relationship of the SC and the PC is invariant; the current vector of the PC is invariant, which leads to an invariant active power of the PC; the load power requirement is provided by the grid sources, PC and SC; and the energy of the SC and PC is from the storage and DC/DC converter.

Define the following:

$$\left|\dot{U}_{sag}\right| = k\left|\dot{U}_s\right| = kU \tag{14}$$

The letter *k* is the sag coefficient and the output voltage vector can be derived as:

$$\begin{aligned}\dot{U}_{series} &= \left|\dot{U}_{series}\right|\angle\beta \\ &= \sqrt{\left|\dot{U}_L\right|^2 + \left|\dot{U}_{sag}\right|^2 - 2\left|\dot{U}_L\right|\cdot\left|\dot{U}_{sag}\right|\cos\gamma}\angle\arctan\frac{\left|\dot{U}_L\right|\sin\gamma}{\left|\dot{U}_L\right|\cos\gamma - \left|\dot{U}_{sag}\right|} \\ &= U\sqrt{1+k^2-2k\cos\gamma}\angle\arctan\frac{\sin\gamma}{\cos\gamma - k}\end{aligned} \tag{15}$$

The sum of the active power from the gird source, SC and PC is given by (16) which is just about the active power consumed by the loads.

$$\begin{aligned}P &= P_s + P_{series} + P_{parallel} \\ &= U_{sag}I_s + U_{series}\cos\beta I_s + U(1-\cos\gamma)I_s \\ &= [U_{sag} + U_{series}\cos\beta + U(1-\cos\gamma)]I_s \\ &= U_s I_s \\ &= UI\cos\varphi\end{aligned} \tag{16}$$

C. UPQC Coordinated Control Optimization Condition

According to the UPQC coordinated control strategy, selecting a suitable angle γ can make the UPQC work in the best condition and realize the capacity optimization allocation to reduce the production cost. The following analyzes the UPQC coordinated control strategy based on the optimal allocation theory in the case of voltage sags.

Ignoring the power losses of the converters and lines, the SC capacity and the PC capacity can be obtained by (17) and (18) according to (6), (9) and (16).

$$\begin{aligned}S_s &= \sqrt{(UI\sin\gamma\cos\varphi)^2 + (UI\sqrt{1+k^2-2k\cos\gamma}\cos\beta\cos\varphi)^2} \\ &= UI\cos\varphi\sqrt{\sin^2\gamma + (1+k^2-2k\cos\gamma)\cos^2\beta}\end{aligned} \tag{17}$$

$$\begin{aligned}S_p &= \sqrt{[UI(\sin\varphi - \sin\gamma\cos\varphi)]^2 + [UI(1-\cos\gamma)\cos\varphi]^2} \\ &= UI\sqrt{\sin^2\varphi - \sin\gamma\sin 2\varphi + 2(1-\cos\gamma)\cos^2\varphi}\end{aligned} \tag{18}$$

$$\beta = \arctan\frac{\sin\gamma}{\cos\gamma - k} \tag{19}$$

Selecting a suitable angle γ can optimize the capacity allocation of the SC and PC to realize a high economic benefit, a low investment cost and a small equipment capacity. Therefore, the objective function of the optimization allocation is defined by the minimum $f(\gamma)$ as:

$$f(\gamma) = \mu_1 S_s + \mu_2 S_p + \mu_3(S_s + S_p) + C \tag{20}$$

μ_1 is the unit capacity price of the SC which can be taken as \$ 500/kVA; μ_2 is the unit capacity price of the PC which can be taken as \$ 400/kVA and it does not consider the harmonic capacity; μ_3 is the unit capacity price of the DC/DC converter which can be taken as \$ 300/kVA; *C* is the fixed cost which is \$ 800; *U*=220V and *I*=50A. Put (17), (18), (19) into (20) and the function expression about γ will be obtained. The function $f(\gamma)$ is at its minimum when *k* or φ changes and the best working condition of the UPQC coordinated control can be obtained by calculating the value γ in the case of a minimal $f(\gamma)$.

D. DC Storage Unit

The main circuit topology of the DC storage unit includes a SCM, a bidirectional DC/DC converter and a discharge unit. The SCM provides energy when there is a voltage sag or instantaneous interruption. The bidirectional DC/DC converter is used to adjust the output voltage. The discharge unit is used to provide an energy release circuit when the DC voltage is higher than the threshold value. The storage capacity depends mainly on the SC compensation fashion, the voltage sag level and the duration. The storage unit selection should take into account the storage capacity and the DC voltage demand. The cost can be determined by calculating the number of super-capacitors required. The storage capacity also determines bidirectional DC/DC converter capacity.

IV. UPQC COORDINATED CONTROL STRATEGY WITHOUT A CIRCULATING CURRENT

A working vectogram is shown in Fig. 2(c) under the UPQC coordinated control strategy without a circulating current. The definition of the variable is the same as Fig. 2(a). When there is no grid-side power quality problem, the SC outputs voltage $\dot{U}_{series}$ which is vertical to the current $\dot{I}_s$ and the PC outputs current $\dot{I}_{parallel}$ which is vertical to the voltage $\dot{U}_L$. Thus, the SC and PC only output reactive power, which avoids an active circulating current. However, the present load voltage U_L will exceed rated voltage *U*. The larger the angle γ, the bigger the voltage U_L. Consider the voltage

fluctuation, $U_L<1.05U$, and the angle $\gamma=17^{\circ}$ when $U_L=1.05U$. Usually, $\gamma_{\max}=15^{\circ}$ and U_L=1.035U in order to leave a margin. When $\varphi\le15^{\circ}$, the system power factor is high and it does not need to compensate the reactive power. When $\varphi>15^{\circ}$, the control strategy can be adopted.

In Fig. 2(c):

$$U_L=\frac{U_s}{\cos\gamma}=\frac{U}{\cos\gamma} \tag{21}$$

$$I_s=\frac{I_L\cos\varphi}{\cos\gamma}=I\frac{\cos\varphi}{\cos\gamma} \tag{22}$$

The SC output voltage $\dot{U}_{series}$ can be obtained by (23) in the UPQC control strategy without a circulating current.

$$\dot{U}_{series}=\left|\dot{U}_{series}\right|\angle90^{\circ}=U_s\tan\gamma\angle90^{\circ}=U\tan\gamma\angle90^{\circ} \tag{23}$$

According to sine theorem, $\frac{I_{parallel}}{\sin\delta}=\frac{I_s}{\sin\delta'}$,

and $\delta'=90^{\circ}-\varphi$.

By combining (21) and (22):

$$I_{parallel}=I_s\frac{\sin\delta}{\sin(90^{\circ}-\varphi)}=\frac{I\cos\varphi}{\cos\gamma}\cdot\frac{\sin\delta}{\cos\varphi}=I\frac{\sin\delta}{\cos\gamma} \tag{24}$$

The PC output current $\dot{I}_{parallel}$ can be derived as:

$$\dot{I}_{parallel}=-\dot{I}_c=I\frac{\sin\delta}{\cos\gamma}\angle(90^{\circ}+\gamma) \tag{25}$$

The active power P_s generated by the grid is given as:

$$P_s=U_s\cdot I_s=UI\frac{\cos\varphi}{\cos\gamma} \tag{26}$$

The active power P_L consumed by the load is given as:

$$P_L=U_L\cdot I_L\cos\varphi=\frac{U}{\cos\gamma}I\cos\varphi=UI\frac{\cos\varphi}{\cos\gamma} \tag{27}$$

According to (26) and (27), P_s=P_L. That is to say, the grid provides active power to the load.

The reactive power Q_c generated by the SC is derived as:

$$Q_c=U_{series}\cdot I_s=U\tan\gamma\frac{I\cos\varphi}{\cos\gamma}=UI\frac{\tan\gamma\cos\varphi}{\cos\gamma} \tag{28}$$

The reactive power Q_p generated by the PC is derived as:

$$Q_p=U_L\cdot I_{parallel}=\frac{U}{\cos\gamma}\cdot\frac{I\sin\delta}{\cos\gamma}=UI\frac{\sin\delta}{\cos^2\gamma} \tag{29}$$

$$Q_c+Q_p=UI\frac{\sin\varphi}{\cos\gamma} \tag{30}$$

The reactive power Q_L consumed by the load is derived as:

$$Q_L=U_L\cdot I_L\sin\varphi=\frac{U}{\cos\gamma}I\sin\varphi=UI\frac{\sin\varphi}{\cos\gamma} \tag{31}$$

(30) and (31) show that reactive power consumed by the load is shared by the SC and the PC. (27) and (31) show that $\cos\gamma$ is close to 1 with a small value of γ. This makes the load active power and reactive power close to $UI\cos\varphi$ and $UI\sin\varphi$, respectively. In fact, an increasing U_L leads to the an increase in the load power. Whereas, the bigger the angle γ, the bigger the reactive power of the SC which can share a greater burden of the PC. In the case of $\varphi=45^{\circ}$ and $\gamma_{\max}=15^{\circ}$, Q_c=0.196UI and Q_p=0.536UI. $\Delta Q=(0.732-0.707)UI=0.025UI$. It can be deduced that the active and reactive power increase by 0.025UI.

TABLE I
SYSTEM ELECTRICAL PARAMETERS

Description	Real value
Nominal line voltage	380V
System frequency	50Hz
Switching frequency	7.2kHz
Resistance load	17Ω
Inductance load	46mH
Nonlinear load	3-phase rectifier+12Ω
Series filter inductor	1mH
Parallel filter inductor	3mH
DC/DC inductor	1mH
Series transformer	17kVA

After determining γ ($\gamma\le\gamma_{\max}=15^{\circ}$) under real working conditions, the SC and PC output can be obtained by (23) and (25) in the UPQC coordinated control strategy without a circulating current. When voltage sags exist, this strategy can be the same as the UPQC strategy with a circulating current in case of voltage sags.

The strategy with a circulating current and the strategy without a circulating current are two different strategies which work in different cases and realize different functions. It is possible to choose either according to the requirements. If a control strategy that switches from one to the other is needed, this can be realized by selecting a corresponding γ and changing the output vectors of the series converter and parallel converter according to the two strategies.

V. SIMULATION AND EXPERIMENTAL VERIFICATION

In order to verify the effectiveness of these strategies, a simulation model and prototype system are constructed. In this section, the simulation results are based on PSIM software and the experimental results are based on a 100kVA three-phase prototype. Table I shows the related electrical parameters of the simulation and experiment. The system uses a step-up transformer (the ratio is 1:2) to debase the current requirement of the SC switches and the filter. The SC and PC capacities are both 50kVA and the capacity of all of the transformers is one-third of the SC capacity (about 17kVA) due to the three-phase system.

The serial filter is an LC filter. When its corner frequency is much lower than the switching frequency, the filter function is obvious in the range of the nearby switching frequency. The switching frequency f_s is 7.2kHz in this system and the corner frequency is designed to be one-tenth of the switching frequency. The ripple current of the filter

inductance ΔI_s is inversely proportional to the inductance and the current is about 15%~25% of the rated current. From the above analysis, (32) and (33) are obtained. U_{DC} is 690V in this system. The filter inductance L_s is 1.27mH according to (32) and (33) and is given as 1mH in order to reduce the voltage drop. The filter capacitance C_s is 48.9uF and is given as 50uF. The design principle of the parallel filter is similar to that of the serial filter and the ripple current is usually 5%~10% of the rated current in order to reduce the harmonic fluctuation range. The filter inductance L_p is given as 3mH.

$$\frac{1}{2\pi\sqrt{L_s C_s}} = 720\text{Hz} \tag{32}$$

$$\Delta I_s = \frac{U_{DC}}{2\times 2L_s f_s} = 25\%\cdot\frac{50\text{kVA}}{3\times 220\text{V}} = 18.9\text{A} \tag{33}$$

A. Simulation Results

According to Fig. 1, the relative simulation parameters are determined. The grid phase voltage is 220V. A voltage sag occurs between 0.1s and 0.2s and the sag value is 30% of the rated voltage. The sampling time is 1e-7s, the power angle φ is about $\pi/4$, and according to (11), $\gamma_{ref} = \pi/6$.

Fig. 3(a) and 3(b) show the simulation results under the UPQC coordinated control with a circulating current. Fig. 3(a) shows the voltage and current waveforms of phase A. During the simulation, the grid voltage Vsa and the current isa are sine characteristic and the angle between Vsa and isa is close to 0, which achieves a unit power factor of grid-side. The load voltage VLa maintains a sine characteristic and normal amplitude during voltage sags. Vca is the SC output voltage, iCa is the PC output current, and iLa is the load current. Fig. 3(b) shows the SC output active and reactive power (Ps and Qs) and the PC output active and reactive power (Pp and Qp). Ps and Pp are almost equal and opposite in direction which is the aforementioned circulating active current. The SC absorbs energy from the storage unit during voltage sags and generates reactive power for compensation. Qs and Qp are kept almost invariable during the simulation which is the same as the theoretical analysis.

Fig. 4(a) and 4(b) show the simulation results under the UPQC coordinated control without a circulating current when there is no voltage sag. The variables are the same as in Fig. 3(a) and 3(b). Fig. 4(a) shows the voltage and current waveforms of phase A. They indicate that the angle between Vsa and isa is close to 0; the load voltage VLa is a little bigger than Vsa; the Vca vector is vertical and lead to the isa vector; and the iCa vector is vertical and lead to the VLa vector. Fig. 4(b) shows the SC output active and reactive power (Ps and Qs), and the PC output active and reactive power (Pp and Qp). Ps and Pp are small and are mostly made up of converter loss. Qs and Qp are kept almost invariable during the simulation and both converters compensate the reactive power.

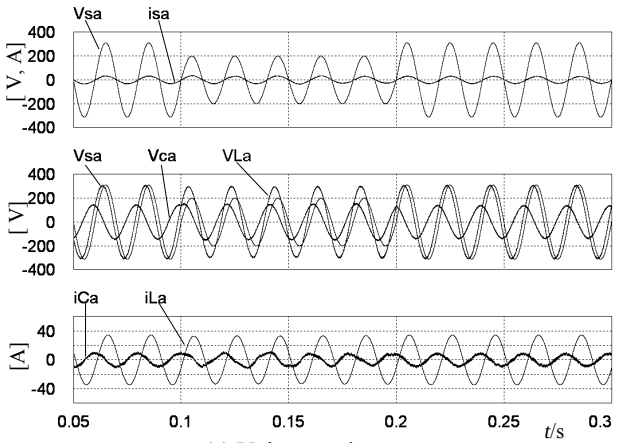

(a) Voltage and current.

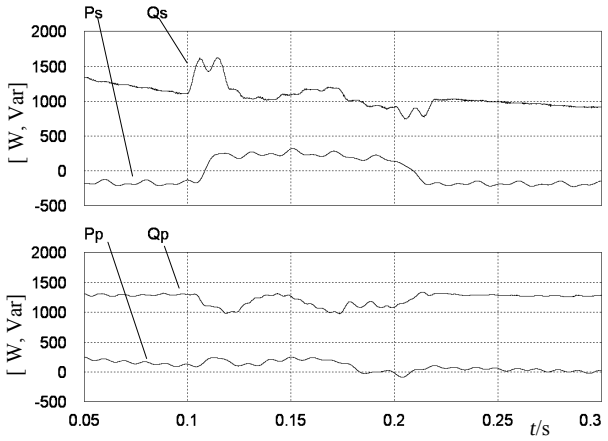

(b) Active and reactive power.

Fig. 3. Simulation waveform under UPQC coordinated control with circulating current.

B. Experimental Results

In this section, a 100kVA three-phase UPQC prototype is designed to verify the UPQC coordinated control strategy. The system control diagram is shown in Fig. 5(a) which includes the control core with a digital signal processor TMS320F28335, a power supply, AC and DC voltage sampling, current sampling, analog digital conversion, a PWM output drive and protection control. The DSP executes the signal processing, mathematical calculations and logic judgment. It then outputs required signals according to the control strategy. These signals include the PWM signal (used by the SC, PC and DC/DC converter), the SCR signal (bidirectional thyristors switching), the KM signal (contactor state control) and the PDP signal (system protection). Fig. 5(b) shows the control structure diagram with a circulating current. $U_s(\omega t)$, $I_L(\omega t)$ and U_{DC} are the grid voltage, load current and common DC voltage. $\dot{U}_C^*$, $\dot{I}_C^*$ and U_{DC}^* are the corresponding reference values. $\dot{U}_C$ is the sampling voltage of the series converter output. $\dot{I}_C$ is the sampling current of the parallel converter output. K_{P1}, K_{P2} and K_{P3} are the corresponding proportional coefficients of the PI

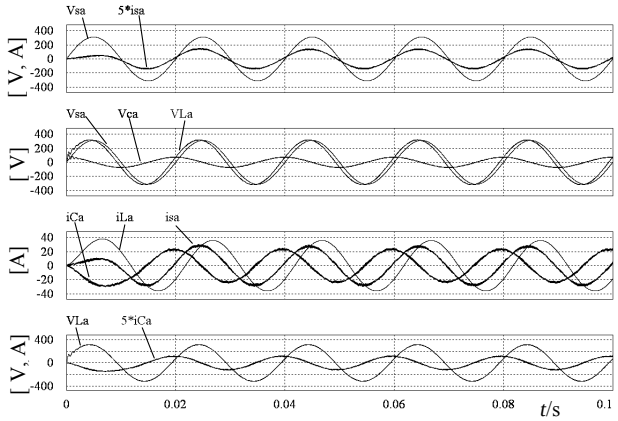

(a) Voltage and current.

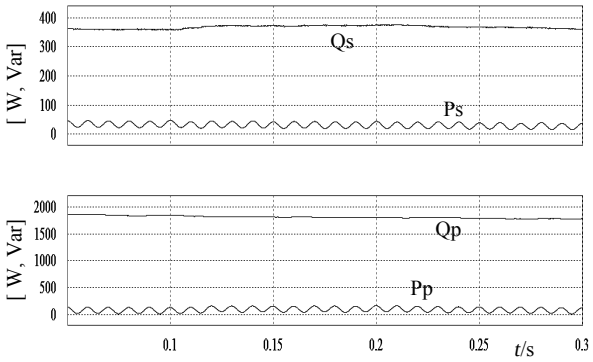

(b) Active and reactive power.

Fig. 4. Simulation waveform under UPQC coordinated control without circulating current.

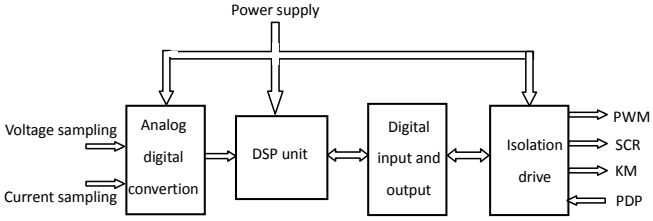

(a) System control diagram.

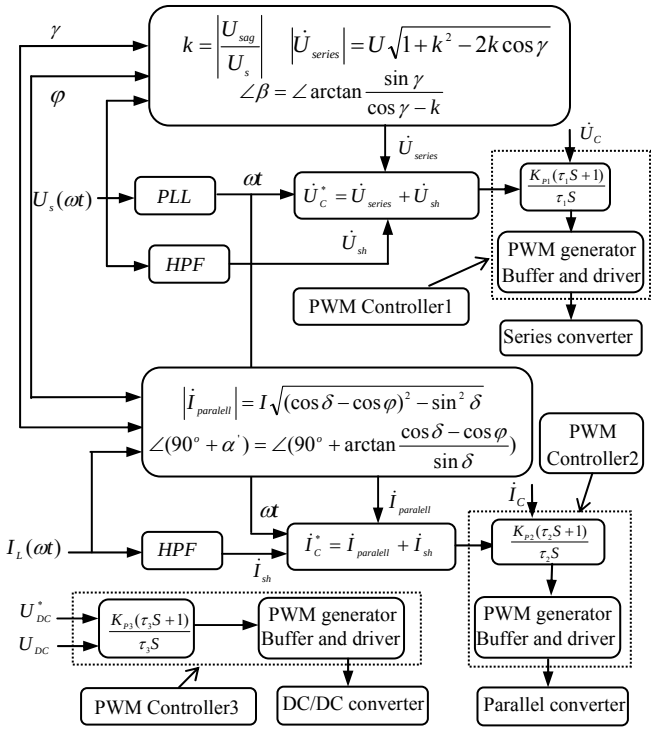

(b) UPQC control structure diagram with circulating current.

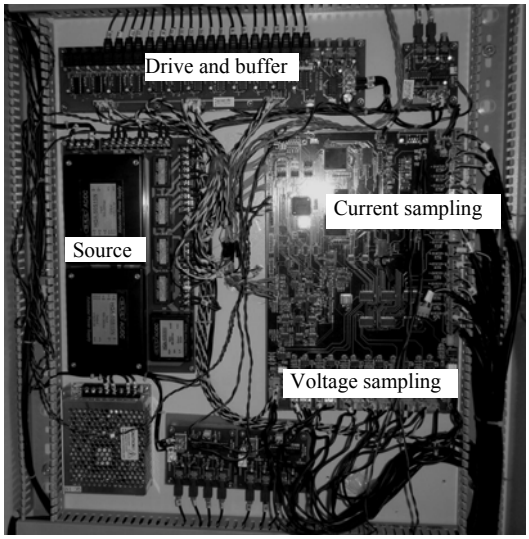

(c) UPQC control system.

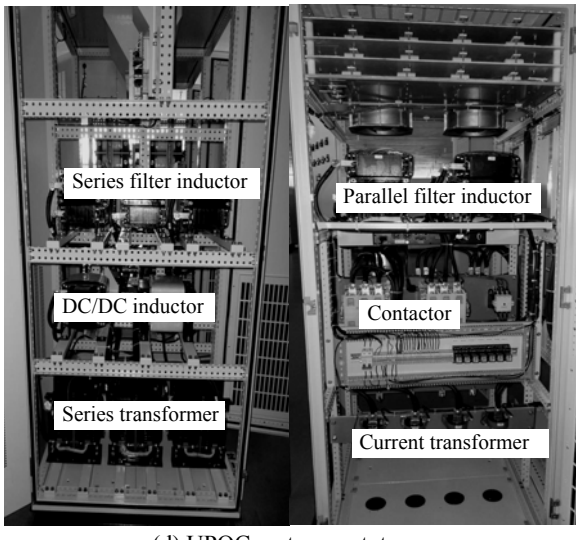

(d) UPQC system prototype.

Fig. 5. UPQC system prototype.

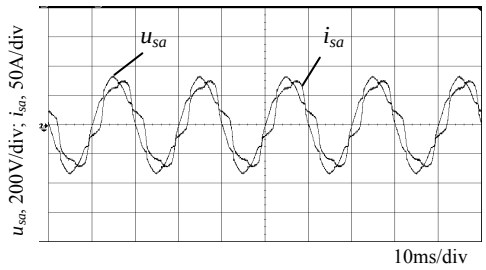

(a) Grid voltage and current waveforms before compensation.

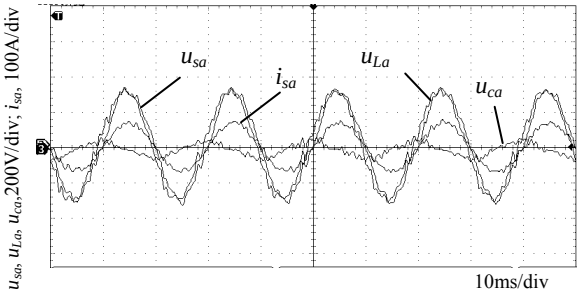

(b) Waveforms after compensation without voltage sags.

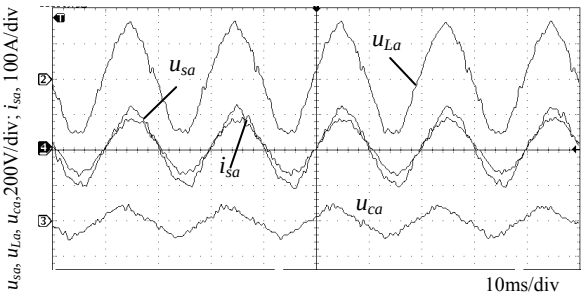

(c) Waveforms after compensation with voltage sags.

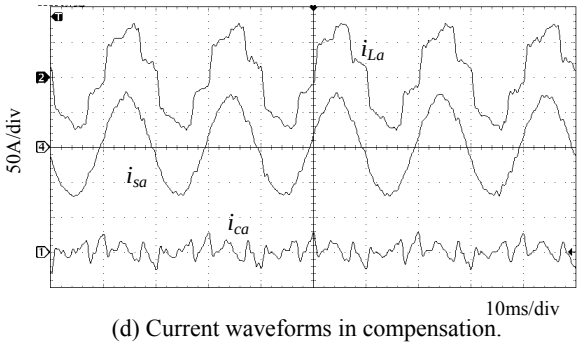

(d) Current waveforms in compensation.

Fig. 6. Experimental waveforms of UPQC coordinated control with circulating current.

regulators. τ_1, τ_2 and τ_3 are the corresponding integral coefficients of the PI regulators. In this paper, K_{P1}=12, K_{P2}=10, K_{P3}=0.05, τ_1=0.01, τ_2=0.02, and τ_3=0.2. The PWM generator uses the triangular wave comparison method. The buffer and driver use 74F245 and M57962 to drive the IGBT. PLL means Phase Lock Loop and HPF means High Pass Filter. $\dot{U}_{sh}$ and $\dot{I}_{sh}$ are the grid voltage and load current harmonic component. The other variables are the same as aforementioned. Fig. 5(c) and 5(d) are the UPQC control system and the main circuit system, respectively.

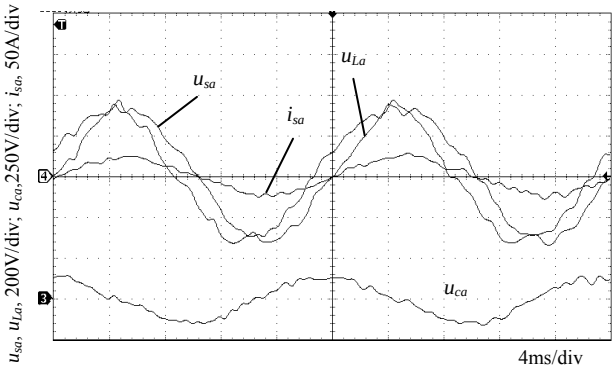

(a) Voltage and current waveforms without voltage sags.

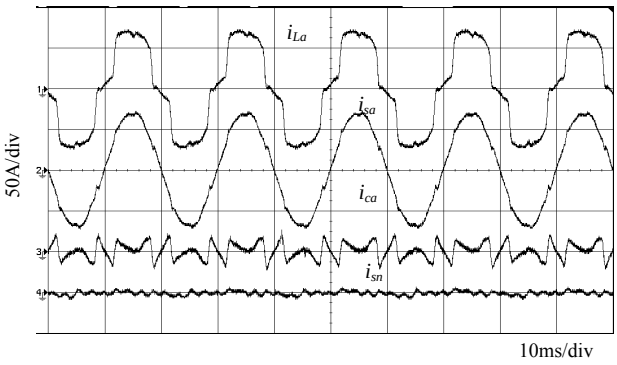

(b) Current waveforms without voltage sags.

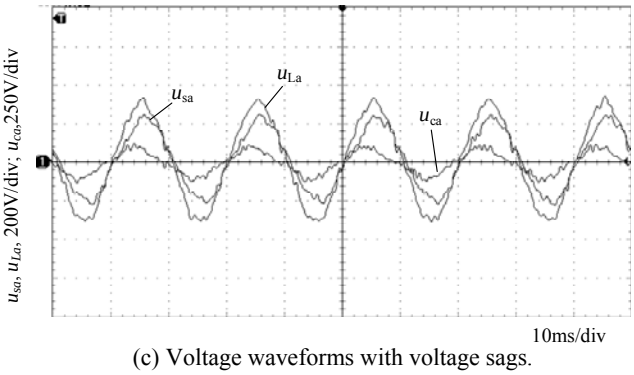

(c) Voltage waveforms with voltage sags.

Fig. 7. Experimental waveforms of UPQC coordinated control without circulating current.

Experimental waveforms of the UPQC coordinated control with a circulating current are shown in Fig. 6(a), 6(b), 6(c) and 6(d) which take phase A as an example. The grid voltage u_{sa} and grid current i_{sa} waveforms before compensation indicate that i_{sa} possess severe harmonics and that the system needs reactive power compensation. Fig. 6(b) includes waveforms after compensation without voltage sags, which indicate that the angle between u_{sa} and i_{sa} is nearly 0 and that the grid-side power factor is nearly 1 through the reactive compensation of the SC and PC. u_{La} and u_{ca} are the load voltage and the SC output voltage, respectively. Under voltage sags (about 20% of the rated voltage), the u_{sa}, i_{sa}, u_{La}, and u_{ca} waveforms in Fig. 6(c) show that the system maintains a high power factor and that u_{La} maintains a normal value during voltage sags. i_{La} and i_{ca} in Fig. 6(d) are the load

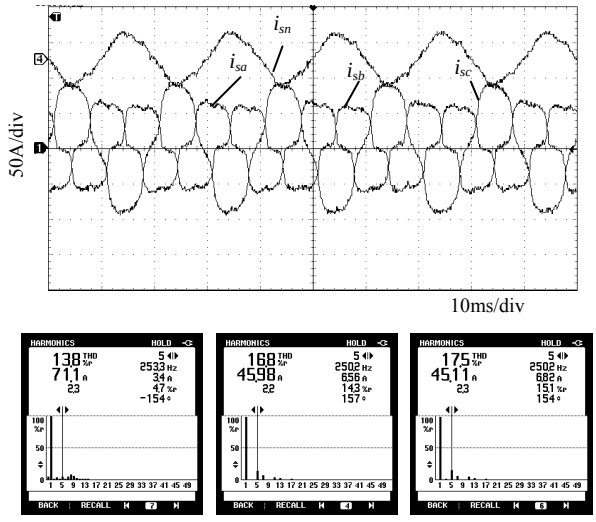

(a) Grid current waveforms and THD without UPQC.

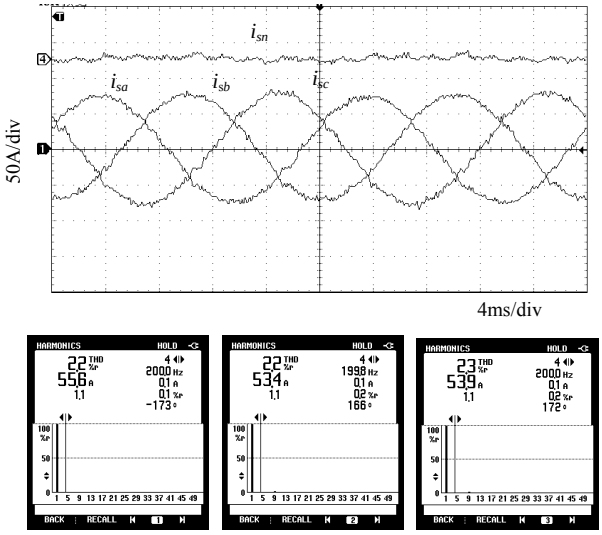

(b) Grid current waveforms and THD with UPQC working.

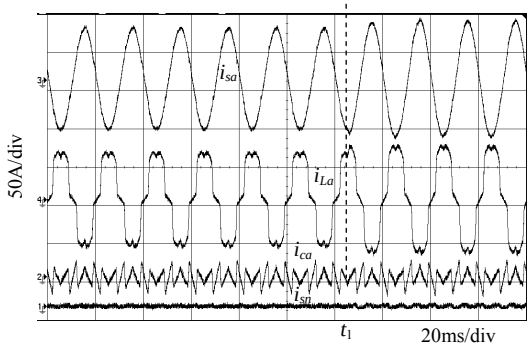

(c) Current waveforms when loads change abruptly.

Fig. 8. Current experimental waveforms.

current and the PC output current, respectively.

Experimental waveforms of the UPQC coordinated control without a circulating current are shown in Fig.7(a), 7(b) and 7(c) which take phase A as an example. Under the control, the grid-side power factor is kept high and the SC output voltage u_{ca} vector is vertical to the gird current i_{sa} vector. The grid-side neutral current i_{sn} is nearly 0. Regardless of whether voltage sags occur or not, u_{La} maintain a normal value.

Fig. 8(a) and 8(b) show grid current waveforms and THDs (total harmonic distortions) of the PC in the case of the UPQC working and not working. There exists a severe load imbalance. When the UPQC does not work, the THDs of the three-phase current i_{sa}, i_{sb} and i_{sc} are 13.8%, 16.8% and 17.5%, respectively, and the neutral current i_{sn} is large. After the UPQC compensation, the THDs of the three-phase current i_{sa}, i_{sb} and i_{sc} are 2.2%, 2.2% and 2.3%, respectively, and the neutral current i_{sn} is nearly zero. The three-phase currents are nearly simple and the imbalance problem is resolved. Fig.8(c) shows the current waveforms in the case of an abrupt load change (the resistance load in TABLE I was abruptly changed from 17Ω to 12Ω at t_1). It can be found that the proposed strategy does not influence the other functions of the UPQC and responds quickly from the waveforms.

The simulation and experimental results verify that the UPQC coordinated control strategy with and without a circulating current can improve the power quality problems, and use the SC to compensate the reactive power. Through rational capacity allocation between the SC and the PC, the strategy realizes coordinated control among the SC, PC and DC storage unit.

VI. CONCLUSIONS

This paper presented a novel UPQC coordinated control strategy with and without a circulating current according to the UPQC running feature. The strategies unite the reactive power allocation strategy of the SC and PC, the composite control strategy of the SC and the compensation strategy of the DC storage unit which effectively solves the SC long term idle problem. The best working condition of the UPQC under the proposed strategies is deduced to optimize all of the UPQC units and reduce the production cost. Meanwhile, the strategies can be properly adjusted according to different customer needs, especially in the case of high power quality equipment to meet different norms. The strategies theory, simulation results and experimental results show that both of the strategies can feasibly improve the power quality problems and coordinately allocate the capacity output of the SC and PC.

ACKNOWLEDGMENT

This work was supported by National High Technology Research and Development of China (863 Programme) (2012AA050213), National Natural Science Foundation of China under Project 51177096, 51207170, 61271001 and Fundamental Research Funds for the Central Universities under Project 14CX02085A, 13CX02101A.

REFERENCES

[1] V. Khadkikar, "Enhancing electric power quality using UPQC: A comprehensive overview," *IEEE Trans. Power Electron.*,Vol. 27, No. 5, pp. 2284-2297,May. 2012.

[2] A. Teke, L. Saribulut, and M. Tumay, "A novel reference signal generation method for power-quality improvement of unified power-quality conditioner," *IEEE Trans. Power Del.*, Vol. 26, No. 4, pp. 2205-2214, Apr. 2011.

[3] M. Brenna, R. Faranda, E.Tironi,"A new proposal for power quality and custom power improvement: open UPQC," *IEEE Trans. Power Del.*, Vol. 24, No. 4, pp. 2107-2116, Apr. 2009.

[4] B. Han, B. Bae, S. Baek, and G. Jang, "New configuration of UPQC for medium-voltage application," *IEEE Trans. Power Del.*, Vol. 21,No. 3, pp. 1438-1444, Mar. 2006.

[5] I. Axente, J. N. Ganesh, M. Basu, M. F. Conlon, and K. Gaughan, "A 12-kVA DSP-controlled laboratory prototype UPQC capable of mitigating unbalance in source voltage and load current," *IEEE Trans. Power Electron.*, Vol. 25, No. 6, pp. 1471-1479, Jun. 2010.

[6] S. B. Karanki, M. K. Mishra, and B. K. Kumar, "Particle swarm optimization-based feedback controller for unified power-quality conditioner," *IEEE Trans. Power Del.*, Vol. 25, No. 4, pp. 2814-2824, Oct. 2010.

[7] M. Gómez, E. Jiménez, E. Martínez-Cámara, M. Pérez, and J. Blanco, "LVRT- DGFACTS devices in wind farms," in *Proc. Power Engineering, Energy and Electrical Drives Conf*., pp. 1-7, 2011.

[8] Y. Li, D. M. Vilathgamuwa, and P. C. Loh, "Microgrid power quality enhancement using a three-phase four-wire grid-interfacing compensator," *IEEE Trans. Ind. Appl.*, Vol. 41, No. 6, pp. 1707-1719, Jun. 2006.

[9] V. G. Kinhal, P. Agarwal, and H. O. Gupta, "Performance investigation of neural-network-based unified power-quality conditioner," *IEEE Trans. Power Del.*, Vol. 26, No. 1, pp. 431-437, Jan. 2011.

[10] J. A. Muñoz, J. R. Espinoza, L. A. Moran, and C. R. Baier, "Design of a modular UPQC configuration integrating a components economical analysis," *IEEE Trans. Power Del.*, Vol. 24, No. 4, pp. 1763-1772, Apr. 2009.

[11] V. Khadkikar and A. Chandra, "A novel structure for three-phase four-wire distribution system utilizing unified power quality conditioner (UPQC)," *IEEE Trans. Ind. Appl.*, Vol. 45, No. 5, pp. 1897-1902, May. 2009.

[12] H. R. Mohammadi, A. Y. Varjani, and H. Mokhtari, "Multiconverter unified power-quality conditioning system: MC-UPQC," *IEEE Trans. Power Del.*, Vol. 24, No. 3, pp. 1679-1686, Jul. 2009.

[13] A. E. Leon, S. J. Amodeo, J. A. Solsona, and M. I. Valla, "Non-linear optimal controller for unified power quality conditioners," *IET power Electron*., Vol. 4, No. 4, pp. 435-446, Apr. 2011.

[14] N. G. Jayanti, M. Basu, M. F. Conlon, and K. Gaughan, "Rating requirements of the unified power quality conditioner to integrate the fixedspeed induction generator-type wind generation to the grid," *IET Renew Power Gener*., Vol. 3, No. 2, pp. 133-143, Feb. 2009.

[15] V. Khadkikar, A. Chandra, A. O. Barry, and T. D. Nguyen, "Power quality enhancement utilising single-phase unified power quality conditioner: digital signal processor-based experimental validation," *IET power Electron*., Vol. 4, No. 3, pp. 323-331, Mar. 2011.

[16] L. Zhang, P. C. Loh, and F. Gao, "An integrated nine-switch power conditioner for power quality enhancement and voltage sag mitigation," *IEEE Trans. Power Electron.*, Vol. 27, No. 3, pp. 1177-1190, Mar. 2012.

[17] Y. Lu, G. Xiao, B. Lei, X. Wu, and S. Zhu, "A transformerless active voltage quality regulator with the parasitic boost circuit," *IEEE Trans. Power Electron.*, Vol. 29, No. 4, pp. 1746-1756, Apr. 2014.

[18] T. Jimichi, H. Fujita, and H. Akagi, "A dynamic voltage restorer equipped with a high-frequency isolated DC-DC converter," *IEEE Trans. Ind. Appl.*, Vol. 47, No. 1, pp. 169-175, Jan. 2011.

[19] M. Basu, S. P. Das, and G. K. Dubey, "Investigation on the performance of UPQC-Q for voltage sag mitigation and power quality improvement at a critical load point," *IET Gener. Transm. Distrib*., Vol. 2, No. 3, pp. 414-423, Mar. 2008.

[20] W. C. Lee, D. M. Lee, and T.-K. Lee, "New control scheme for a unified power-quality compensator-Q with minimum active power injection," *IEEE Trans. Power Del.*, Vol. 25, No. 2, pp. 1068-1076, Feb. 2010.

[21] M. Kesler and E.Ozdemir, "Synchronous-reference-frame-based control method for UPQC under unbalanced and distorted load conditions," *IEEE Trans. Ind. Electro.*, Vol. 58, No. 9, pp. 3967-3975, Sep. 2011.

[22] G. S. Kumar, P. H. Vardhana, B. K. Kumar, and M. K. Mishra, "Minimization of VA loading of unified power quality conditioner (UPQC)," in *POWERENG 2009 conf*., pp. 552-557, Mar. 2009.

[23] V. Khadkikar and A. Chandra, "UPQC-S: A novel concept of simultaneous voltage sag/swell and load reactive power compensations utilizing series inverter of UPQC," *IEEE Trans. Power Electron.*, Vol. 26, No. 9, pp. 2414-2425, Sep. 2011.

[24] V. Khadkikar and A. Chandra, "A new control philosophy for a unified power quality conditioner (UPQC) to coordinate load-reactive power demand between shunt and series inverters," *IEEE Trans. Power Del.*, Vol. 23, No. 4, pp. 2522-2534, Oct. 2008.

[25] H. Heydari and A. H.Moghadasi, "Optimization scheme in combinatorial UPQC and SFCL using normalized simulated annealing," *IEEE Trans. Power Del.*, Vol. 26, No. 3, pp. 1489- 1498, Mar. 2011.

Xing-tian Feng was born in China, in 1978. He received his B.S. degree in Electrical Engineering and his M.S. degree in Control Theory and Control Engineering from the China University of Petroleum, Dongying, China, in 2001 and 2004, respectively. He received his Ph.D. degree from the Institute of Electrical Engineering, Chinese Academy of Sciences, Beijing, China, in 2012. Since 2004, he has worked as a teacher in the College of Information and Control Engineering, China University of Petroleum, Qingdao, China. His current research interests include power electronics and control, power quality, distributed generation and energy storage technology.

Zhi-hua Zhang was born in China, in 1977. He received his B.S. degree from the Shijiazhuang Railway Institute, Shijiazhuang, China, his M.S. degree from the China University of Petroleum, Dongying, China, and his Ph.D. degree from Shandong University, Jinan, China, in 2001, 2004 and 2012, respectively. He has about ten years of teaching and research experience at the Information and Control Engineering College, China University of Petroleum, Qingdao, China. He is an Associate Professor in the Department of Electrical Engineering, China University of Petroleum. His current research interests include power distribution systems, active voltage control technology, and fault seamless self-healing technology.